SUPPORTING INFORMATION

A Dual-Path Pulse-Echo Instrument for Speed of Sound of Liquids and Measurements on *p*-Xylene and Four Halogenated-Olefin Refrigerants [R1234yf, R1234ze(E), R1233zd(E), and R1336mzz(Z)][1]

Mark O. McLinden*, Richard A. Perkins

Applied Chemicals and Materials Division
National Institute of Standards and Technology
325 Broadway, Mailstop 647.08, Boulder, Colorado 80305 USA

This Supporting Information section presents additional figures showing details of the instrument. All measured values from which the average values reported in the tables were calculated and details on the uncertainties for each measured point are presented as txt files.

List of Figures

* Corresponding author; mark.mclinden@nist.gov

List of Tables—Detailed Experimental Information

(contained in zip file in tab-delimited format)

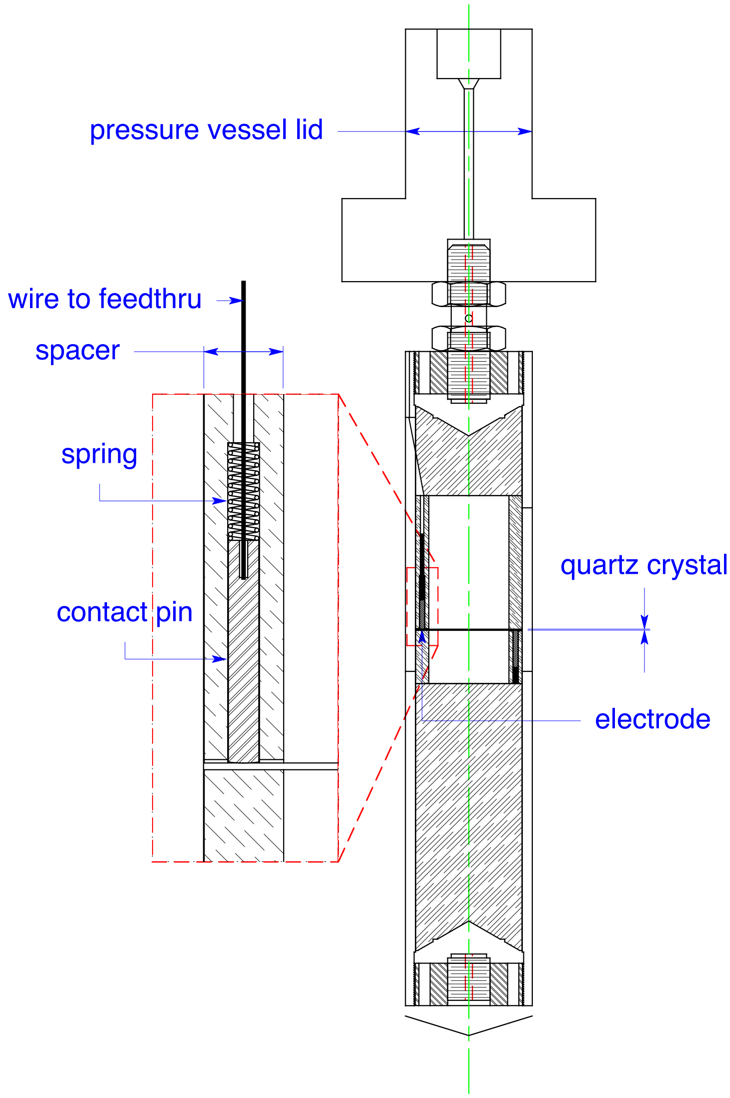

Fig. S1. Detail of the electrical contact to the quartz crystal.

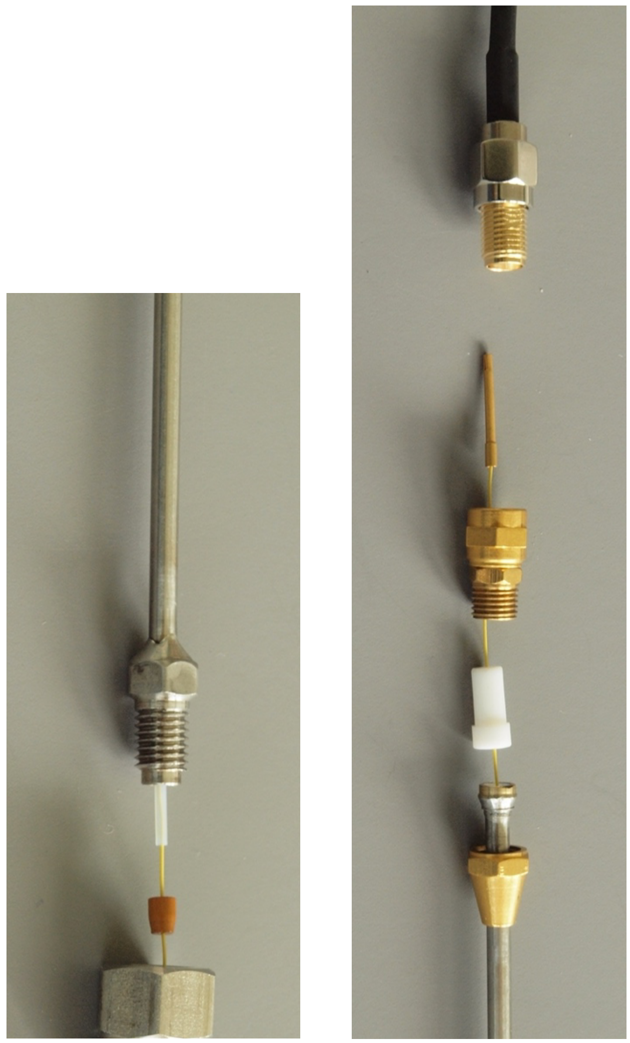

Fig. S2. Photograph of the electrical feedthrough; left: lower portion; right: upper portion.

Pressure vessel for NIST pulse-echo instrument
modified HiP model GC1:
1.125" bore, 6.50" deep from top of main body
HF4 fitting on cap
HF2 fitting at bottom
inside of cap, tapped 7/16-20

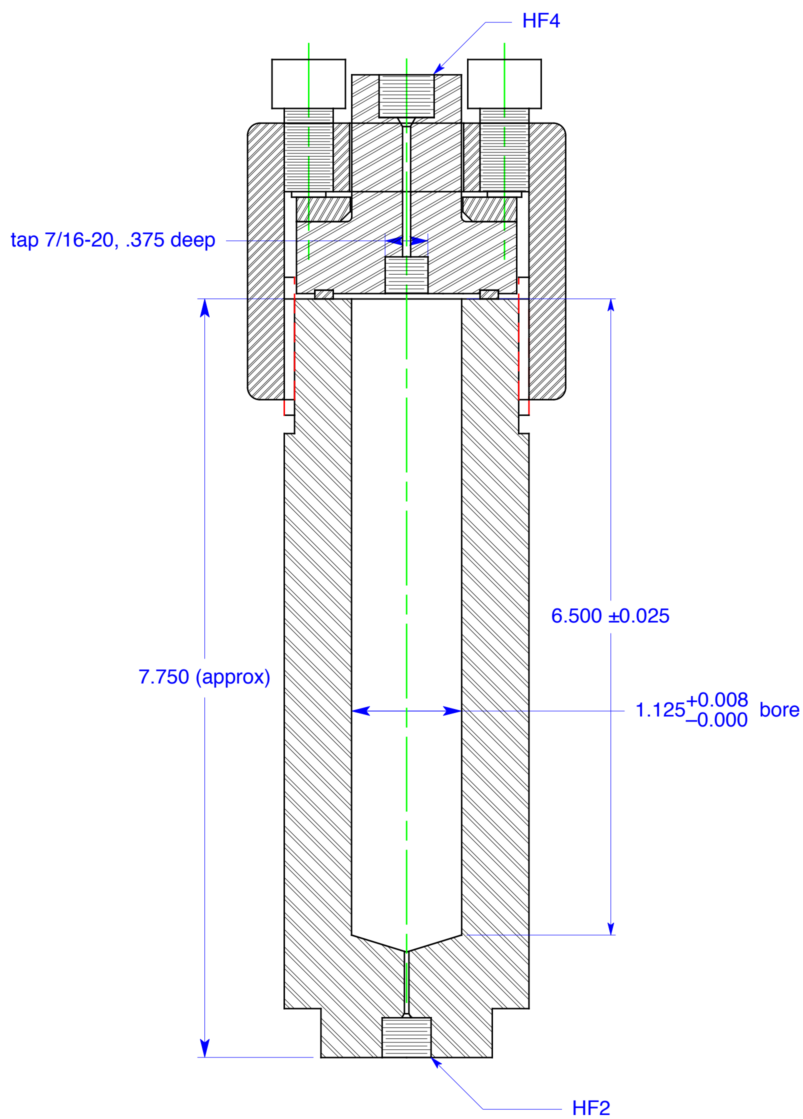

Fig. S3. Cross section of the pressure vessel (custom version of High Pressure Equipment Company model GC1); material is type 316 stainless steel; dimension are in inches.

Fig. S4 Photograph of the thermostatic bath and pressure/filling manifold; the vacuum system is to the left..

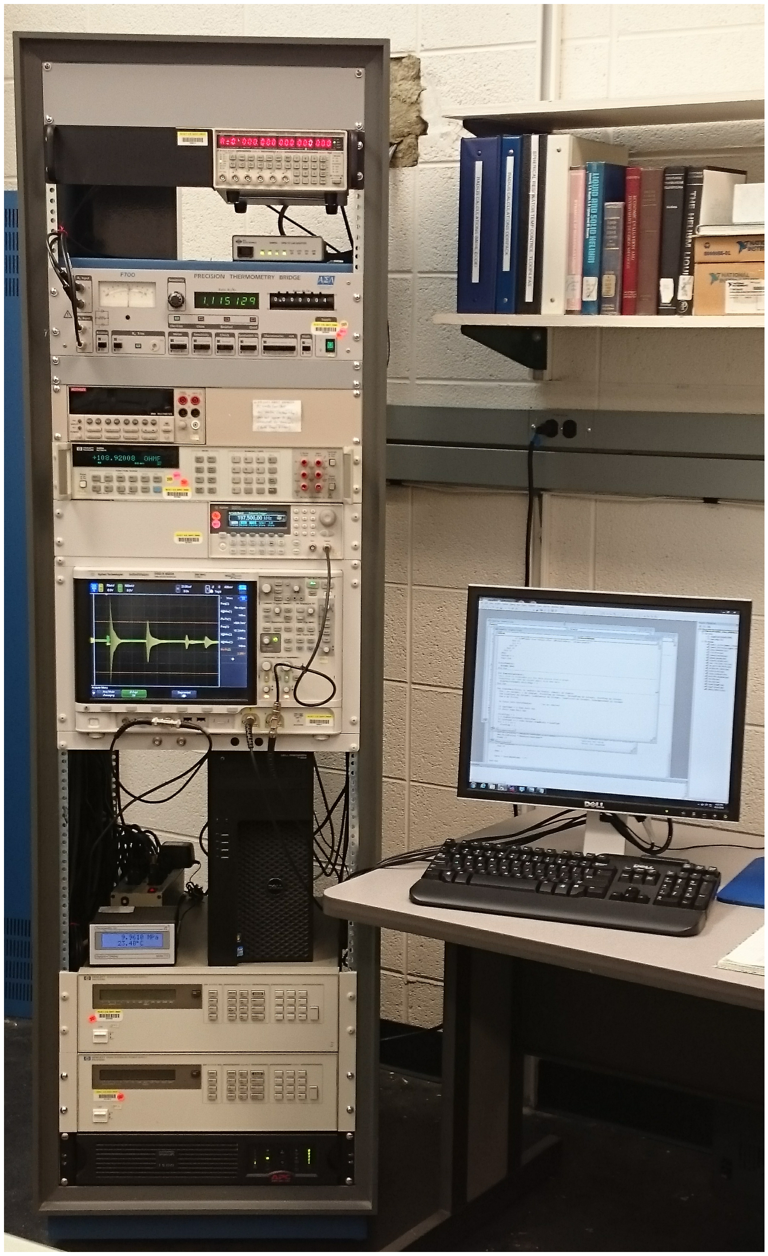

Fig. S5.   Photograph of the electronics rack.

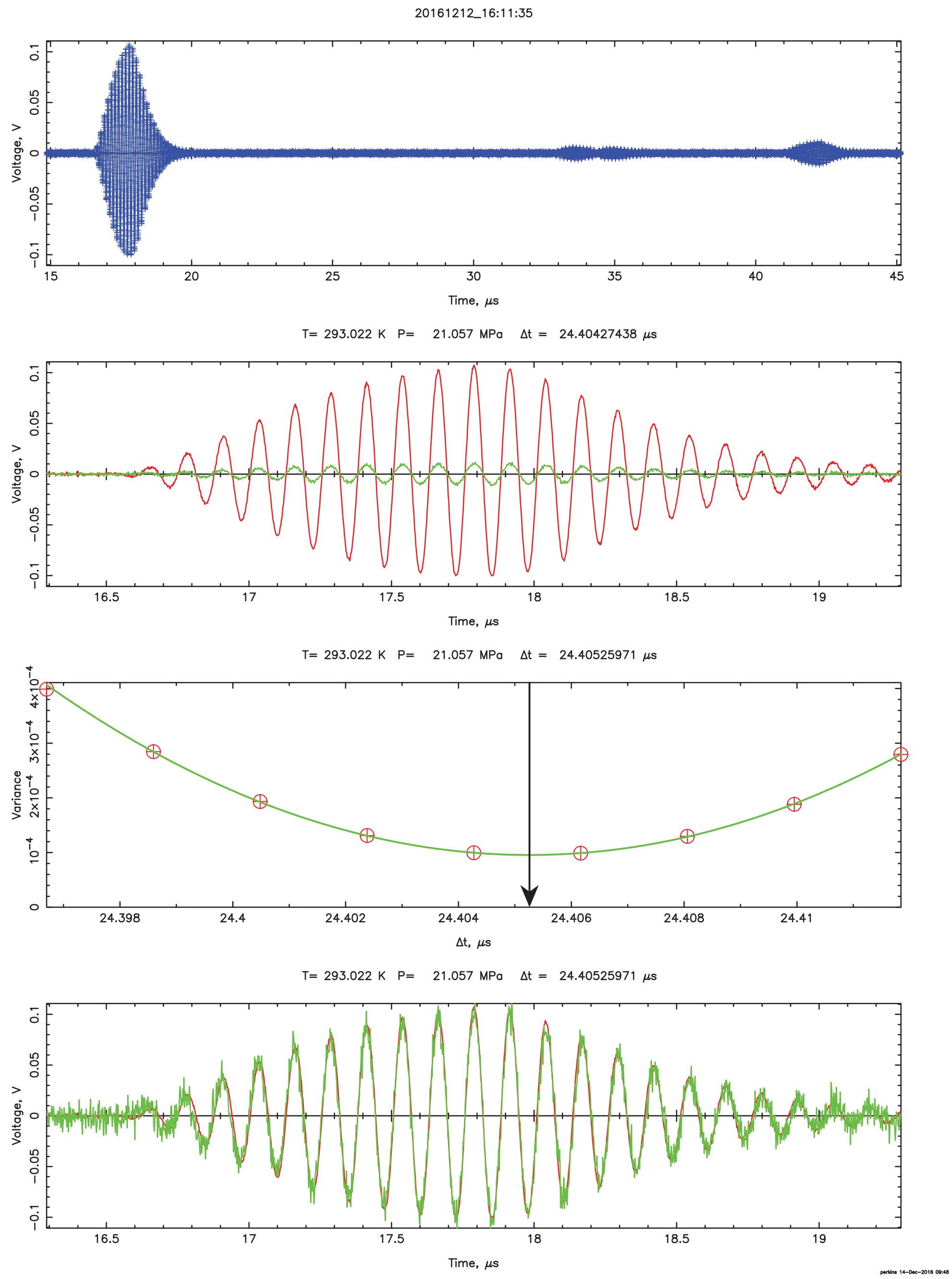

Fig S6. Example of weak echo signals; shown is POE-7 (pentaerythritol tetraheptanoate, $C_{33}H_{60}O_8$, CAS # 25811-35-2) at $T = 293$ K, $p = 21$ MPa from Bruno et al.[2].

---

[2]Bruno, T. J.; Fortin, T. J.; Huber, M. L.; Laesecke, A.; Lemmon, E. W.; Mansfield, E.; McLinden, M. O.; Outcalt, S. L.; Perkins, R. A.; Urness, K. N.; Widegren, J. A. *Thermophysical Properties of Polyol Ester Lubricants*; Natl. Inst. Stand. Technol. Report 8263: 2019.

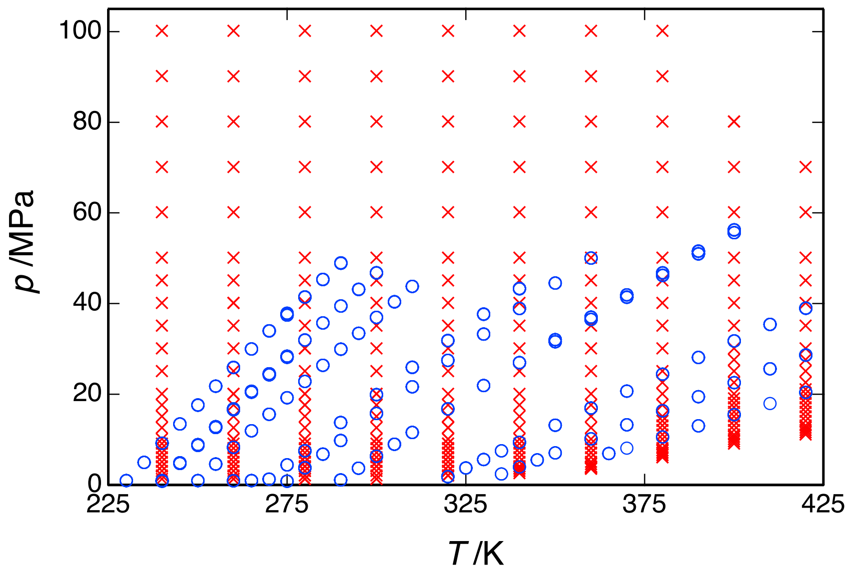

Fig S7. Measured speed-of-sound data for propane; ×, data of Meier[3]; ○, present data.

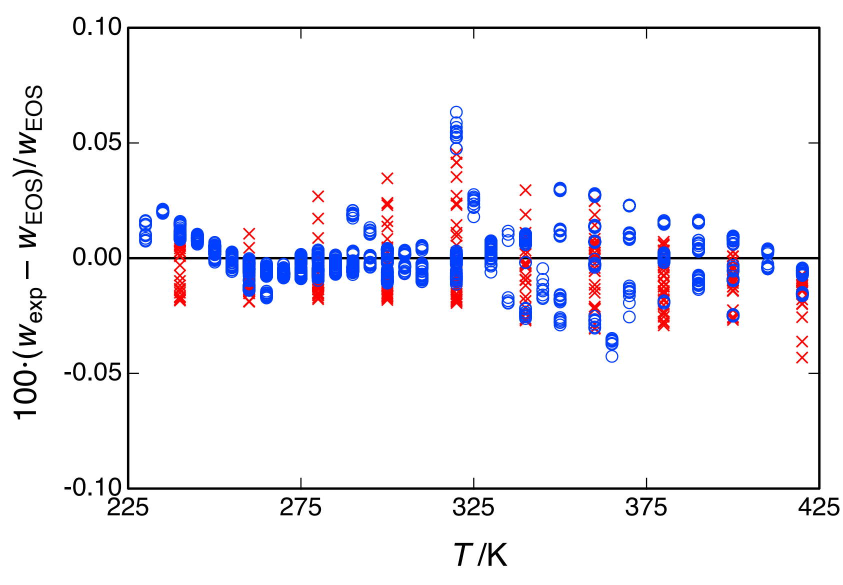

Fig S8. Deviations of propane speed-of-sound data from EOS of Lemmon et al.[4]; ×, data of Meier[3]; ○, present data.

---

[3] Meier, K.; Kabelac, S., Thermodynamic Properties of Propane. IV. Speed of Sound in the Liquid and Supercritical Regions. J. Chem. Engr. Data 2012, 57, 3391-3398.

[4] Lemmon, E. W.; Wagner, W.; McLinden, M. O., Thermodynamic properties of propane. III. Equation of state. Journal of Chemical and Engineering Data 2009, 54, 3141-3180.

Tables S1 – S6: Nomenclature.

Note: The data files in the Supplemental Information are tab-delimited text files. A "#" character in column 1 indicates a comment or other non-data line. The data columns are as follows:

Heading	Explanation
year mo dy	date in format: yyyy mm dd
time	time in format: hh:mm
elapsed hr	elapsed time (hours) since start of isochore or isotherm
T(K)	temperature T/K
p(MPa)	pressure p/MPa, including hydrostatic head correction
w(m/s)	speed of sound w/m·s^{-1}, including diffraction correction
sigma_T	standard deviation in the temperature readings (K) taken before, during, and after a given set of 3 replicate echoes (see Section 2.6); this is a measure of the steadiness of the experimental conditions
sigma_p	standard deviation in the pressure readings (MPa) taken before, during, and after a given set of 3 replicate echoes; this is a measure of the steadiness of the experimental conditions
sigma_w	standard deviation in the sound speed determined from the 3 replicate echoes; large values here (> 0.01 m·s^{-1}) may indicate that the Δt of one or more of the echoes may be in error by an integer number of cycles
N_temp	number of temperatures and pressures recorded (normally 4 for 3 replicate echoes)
N_echo	number of replicate echo signals recorded for a given T and p
w_EOS	speed of sound calculated by the equation of state referenced in the manuscript; note: for p-xylene, this is the EOS of Zhou et al., rather than the empirical fit presented in the manuscript
del_EOS(%)	relative difference between the measured speed of sound and that calculated by the EOS: 100*(w – w_EOS)/w_EOS
Tbath	bath temperature (K) as recorded by the internal temperature sensor; this sensor was located away from the measuring cell, and the "T(K)" above should be used as the sample temperture
dp/dT(%/hr)	relative drift in the pressure over the time for the 3 replicate echo signals; this is a measure of the steadiness of the experimental conditions
u_T/K	combined standard uncertainty in temperature, including Type A uncertainties and PRT and bath gradient effects
u_p/MPa	combined standard uncertainty in pressure, including Type A uncertainties and transducer and hydrostatic head effects
u_w(m.s-1)	standard uncertainty in speed of sound
Uc(%)	relative combinded expanded uncertainty in speed of sound